

# Dalton Transactions

Accepted Manuscript



This is an *Accepted Manuscript*, which has been through the Royal Society of Chemistry peer review process and has been accepted for publication.

*Accepted Manuscripts* are published online shortly after acceptance, before technical editing, formatting and proof reading. Using this free service, authors can make their results available to the community, in citable form, before we publish the edited article. We will replace this *Accepted Manuscript* with the edited and formatted *Advance Article* as soon as it is available.

You can find more information about *Accepted Manuscripts* in the [Information for Authors](#).

Please note that technical editing may introduce minor changes to the text and/or graphics, which may alter content. The journal's standard [Terms & Conditions](#) and the [Ethical guidelines](#) still apply. In no event shall the Royal Society of Chemistry be held responsible for any errors or omissions in this *Accepted Manuscript* or any consequences arising from the use of any information it contains.

## ARTICLE

# Efficient Enhancement of Magnetic Anisotropy by Optimizing Ligand-Field in a Typically Tetranuclear Dysprosium Cluster

Cite this: DOI: 10.1039/x0xx00000x

Received 00th January 2012,  
Accepted 00th January 2012

DOI: 10.1039/x0xx00000x

www.rsc.org/

Jiang Liu, Yan-Cong Chen, Zhong-Xia Jiang, Jun-Liang Liu, Jian-Hua Jia,\* Long-Fei Wang, Quan-Wen Li, and Ming-Liang Tong\*

The perturbation to ligand field around the lanthanide ion may significantly contribute to the magnetic dynamics of single molecule magnet. This can be demonstrated by two typically Dy<sub>4</sub> cluster-based single molecular magnets (SMMs), [Dy<sub>4</sub>X<sub>2</sub>(μ<sub>3</sub>-OH)<sub>2</sub>(μ-OH)<sub>2</sub>(2,2-bpt)<sub>4</sub>(H<sub>2</sub>O)<sub>4</sub>]X<sub>2</sub>·2H<sub>2</sub>O·4EtOH (X = Cl and Br for **1** and **2**, respectively), which were constructed by using 3,5-bis(pyridin-2-yl)-1,2,4-triazole (2,2-bptH) as the polynuclear-chelating ligand. Alternating-current (ac) magnetic susceptibility measurements show that the energy barriers in complexes **1** and **2** were immensely enhanced by comparing with our previous work due to the optimization of the ligand field around Dy<sup>III</sup> ion. Remarkably, their high thermal active barriers with 190 K (**1**) and 197 K (**2**) under zero applied external dc magnetic fields are also among the highest within the reported tetranuclear lanthanide-based SMMs.

## Introduction

As a remarkable class of molecules, Single molecule magnets (SMMs) with magnetic bistability in the field of molecular magnetism have received considerable attention owing to their potential utilities in high density information storage and quantum processing.<sup>1</sup> The fundamental characteristic of these systems is the presence of an energy barrier to the reorientation of magnetization and this can be defined in terms of a large uniaxial anisotropy (*D*) and a large spin ground state (*S*) for transition-metal complexes. In order to maximize the performance of SMMs in practice, the relaxation barrier must be large enough to guarantee stability of the moment orientation to thermal and quantum fluctuations.<sup>2</sup> Hence much effort for questing high barriers in the preceding years is mainly focus on the anisotropic transition metal clusters with large *S* values.<sup>3</sup> Since the discovery of (Bu<sub>4</sub>N)[Tb(Pc)<sub>2</sub>] (H<sub>2</sub>Pc = phthalocyanine) molecule,<sup>4</sup> lanthanide-based single-ion magnets (SIMs) with higher spin reversal barrier started to become as a subject of the extensive research with respect to SMMs.<sup>5</sup> Indeed, for 4f ions the large magnetic moment and strong spin-orbit coupling under the effect of crystal fields can engender much larger single ion magnetic anisotropy when compared with d-block element. It can stabilize the sublevels with the largest *M<sub>J</sub>* values resulting in Ln<sup>III</sup> ions exhibit easy-axis anisotropy (Ising type) and thus higher magnitude of magnetization blocking.<sup>6</sup> Especially for Dy<sup>III</sup>-based SIMs, which always being the focus of study attribute to its usually

large ground Kramers doublet with *M<sub>J</sub>* = 15/2. Subsequent endeavor therefore in the community has primarily been directed at understanding and enhancing uniaxial anisotropy of Dy<sup>III</sup>-containing SIMs.<sup>7</sup> Even so, recent studies have shown that only a few 4f-based SIMs remains keeping large effective energy (*U<sub>eff</sub>*) in the absence of an applied magnetic field due to the fast quantum tunnelling of magnetization (QTM) between ground states.<sup>5c,6a</sup> The documented effective solution for suppressing QTM is strict site symmetry of geometry, such as the well-known quasi-*D<sub>5h</sub>*,<sup>8</sup> *D<sub>4d</sub>*<sup>6a</sup> and *C<sub>3</sub>*<sup>5c</sup> configuration, which depends closely on the ligands around lanthanide ions. But assembling a targeted and perfect symmetry is always a challenging task because of the essence of large coordination number for lanthanides ions.<sup>9</sup> Fortunately, it has proved that QTM can also be reduced moderately by implanting strong magnetic exchange into polynuclear dysprosium SMMs when lack of symmetry environment.<sup>10</sup> The anisotropic axis of Dy<sup>III</sup> ion in this case is often determined by a short coordination bond,<sup>11</sup> whether in SIMs or polynuclear SMMs, for which the origin of magnetic relaxation is found to be the single ion in nature rather than magnetic exchange, verified already by advanced *ab initio* calculations.<sup>6b</sup> In addition, the effective barrier of SMM can be further improved by tuning or optimizing surrounding ligand field of anisotropic axis.<sup>12</sup> Of notable importance is recent work illustrating the effect of electron withdrawing groups on terminally coordinated ligands capable of fine tuning the anisotropic barrier.<sup>12b</sup> It has underlined

that ligand field plays an important role in determining the magnetic anisotropy of Dy<sup>III</sup>-based SMM.

Tetranuclear dysprosium (Dy<sub>4</sub>) cluster has long occupied a vital position in lanthanide-based clusters because of their multifunctional potential and attractive SMM performance.<sup>13</sup> We have previously synthesized a series of typically Dy<sub>4</sub> clusters as well as Dy<sub>8</sub> and Dy<sub>10</sub> clusters by employing (3,5-bis(pyridin-2-yl)-1,2,4-triazole (2,2-bptH) as ligand with different dysprosium salts, which display chirality, fluorescence, ferroelectric, toroidal magnetic moment as well as SMM behavior under different ligand fields.<sup>13a,14</sup> Despite the lack of perfect symmetry for individual Dy<sup>III</sup> ion, QTM still to some extent obtains suppression by magnetic exchange within cluster. It has been proved that deeply investigation to a certain system is undoubtedly important for scientific research.<sup>4,6a,15</sup> In this system, we found that a stable Dy<sub>4</sub> skeleton can be easily formed in a proper alkaline environment. Meanwhile, the anisotropic axis evidenced in such Dy<sub>4</sub> type was close to the orientation of the shortest Dy-O bond upon preceding *ab initio* calculation.<sup>14b</sup> It is worth noting that the solvent molecules or anions coordinated to dysprosium ions are replaceable and thus provide possibility for optimizing ligand field to improve magnetic anisotropy. In this work, two such typical Dy<sub>4</sub> clusters,

[Dy<sub>4</sub>X<sub>2</sub>(μ<sub>3</sub>-OH)<sub>2</sub>(μ-OH)<sub>2</sub>(2,2-bpt)<sub>4</sub>(H<sub>2</sub>O)<sub>4</sub>]X<sub>2</sub>·2H<sub>2</sub>O·4EtOH (X = Cl and Br for **1** and **2**, respectively), were successfully synthesized. The magnetic anisotropy of complexes **1** and **2** were promoted dramatically due to the optimization of ligand field for dysprosium ion. In addition, their thermal energy barriers with 190 K (**1**) and 197 K (**2**) under zero external fields are also among the highest within the reported tetranuclear lanthanide-based SMMs.<sup>6b</sup>

## Experimental section

**Materials and Measurements.** The commercially available chemicals and solvents were used and purified by standard procedures. The C, H and N microanalyses were determined using an Elementar Vario-EL CHNS elemental analyzer. IR spectra using KBr pellets were recorded on a Bio-Rad FTS-7 spectrometer. Magnetic susceptibility measurements were performed with a Quantum Design MPMS-XL7 SQUID. Polycrystalline samples of complex **1** and **2** were embedded in vaseline to prevent torquing. Variable temperature (2-300 K) magnetic susceptibility and field dependence of the magnetization at different temperatures measurements on the polycrystalline samples were performed at different magnetic fields. All the ac susceptibility data were collected at zero dc field and 5 Oe ac amplitude. The sample was packed into the cling film, which was then mounted in low-background diamagnetic plastic straws. The data were corrected for the magnetization of the sample holder and the diamagnetism of the constituent atoms using Pascal constants.

### Synthesis.

[Dy<sub>4</sub>Cl<sub>2</sub>(μ<sub>3</sub>-OH)<sub>2</sub>(μ-OH)<sub>2</sub>(2,2-bpt)<sub>4</sub>(H<sub>2</sub>O)<sub>4</sub>]Cl<sub>2</sub>·2H<sub>2</sub>O·4EtOH (**1**): Single crystal of **1** was obtained by the slow diffusion technique. 2,2-H<sub>2</sub>bpt (67 mg, 0.3 mmol) and triethylamine (30 mg, 0.3 mmol)

dissolved in EtOH (5 mL) were placed in a 5mL test tube while another 1mL test tube contained an ethanolic solution of DyCl<sub>3</sub>·6H<sub>2</sub>O (111 mg, 0.3 mmol). The two vessels were inserted into a 30 mL vial filled with EtOH. Colourless block crystals suitable for single-crystal X-ray diffraction were formed after 2 weeks. (**1**, yield ca. 83% based on Dy). Elemental analysis Calcd (%) for C<sub>56</sub>H<sub>72</sub>Cl<sub>4</sub>Dy<sub>4</sub>N<sub>20</sub>O<sub>14</sub>: C 32.95, H 3.55, N 13.72; Found: C 32.72, H 3.26, N 13.58; IR (KBr) for **1**: ν (cm<sup>-1</sup>) = 3400(br), 1607(s), 1473(s), 1407(s), 1341(vs), 1280(m), 1249(vs), 1199(m), 1137(vs), 1091(w), 1036(s), 986(w), 805(m), 751(w), 720(m), 623(m), 465(w).

[Dy<sub>4</sub>Br<sub>2</sub>(μ<sub>3</sub>-OH)<sub>2</sub>(μ-OH)<sub>2</sub>(2,2-bpt)<sub>4</sub>(H<sub>2</sub>O)<sub>4</sub>]Br<sub>2</sub>·2H<sub>2</sub>O·4EtOH (**2**): Single crystal of **2** was obtained by similar method as **1**. 2,2-H<sub>2</sub>bpt (67 mg, 0.3 mmol) and triethylamine (30 mg, 0.3 mmol) dissolved in EtOH (5 mL) were placed in a 5 mL test tube while another 1mL test tube contained an aqueous solution of anhydrous DyBr<sub>3</sub> (120 mg, 0.3 mmol). The two vessels were inserted into a 30mL vial filled with EtOH. Colourless block crystals suitable for single-crystal X-ray diffraction were formed after 4-5 weeks. (**2**, yield ca. 76% based on Dy). Elemental analysis Calcd (%) for C<sub>56</sub>H<sub>72</sub>Br<sub>4</sub>Dy<sub>4</sub>N<sub>20</sub>O<sub>14</sub>: C 30.31, H 3.27, N 12.62; Found: C 30.19, H 3.37, N 12.89; IR (KBr) for **2**: ν (cm<sup>-1</sup>) = 3306(br), 1607(s), 1480(s), 1416(m), 1353(vs), 1283(m), 1248(vs), 1203(m), 1133(vs), 1082(m), 989(w), 804(s), 751(w), 728(w), 630(m), 440(w).

**X-ray Crystallography.** Crystal diffraction data was recorded at 150(2) K on a Rigaku R-AXIS SPIDER Image Plate Diffractometer with MoK<sub>α</sub> radiation. The structures were solved by direct methods and all non-hydrogen atoms were refined anisotropically by least square on *F*<sup>2</sup> using the SHELXTL program.<sup>16</sup>

## Results and Discussion

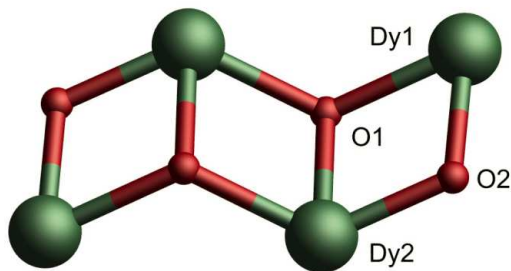
### Crystal Structures.

Single-crystal X-ray crystallography reveals that compounds **1** and **2** are isomorphs hence **1** will be used as a representative example to illustrate their common features. The crystal data are summarized in Table S1 and comprehensive listing of bond lengths and angles for both complexes are given in the supporting information (Table S2).

The molecule structure of **1** has a centro-symmetric defect-dicubane central core as previously reported,<sup>13c,14b</sup> which established by two internal μ<sub>3</sub>-OH groups and two external μ-OH groups based on parallelogram frame of four eight coordinated Dy<sup>III</sup> ions (Figure 1a). The two μ<sub>3</sub>-OH groups were fixed above and below the parallelogram respectively by connecting one Dy1 and two Dy2 atoms with Dy-O bond lengths of 2.342(4), 2.409(4) and 2.427(4) Å and Dy-O-Dy bond angles of 103.31(17), 106.46(17) and 126.20(16)°. It is noted that the μ-OH bridge between Dy1 and Dy2 atoms with short Dy1-O2 and Dy2-O2 contacts of 2.240(4) and 2.252(4) Å was attested meaningful with respect to magnetism. The bond angle of Dy1-O2-Dy2 is 112.76(19)°. In addition, the peripheral four coordination sites of each Dy atom were donated from two 2,2-bptH ligands with Dy-N bond lengths range from

2.428(6) to 2.692(6) Å. The remaining terminal coordination nodes of Dy1 and Dy2 were occupied by H<sub>2</sub>O molecule or H<sub>2</sub>O molecule and Cl (Br) atoms (Figure 1b). The Dy-Cl (Br) bond length is 2.715 (2.889) Å. Calculation of the degree of distortion for the coordination geometries of Dy1 and Dy2 atoms in both compounds by the SHAPE software<sup>17</sup> led to shape measurements close to the triangular dodecahedron (TDD-8) and square antiprism (SAPR-8) with values of 2.031 (2.032) and 1.308 (1.297) respectively. Closing inspection of the packing arrangement by crystallization solvent molecules and Cl (Br) anions reveals stacking of the molecular along the b-axis with intermolecular Dy<sup>III</sup>–Dy distances of 8.98 Å.

(a)



(b)

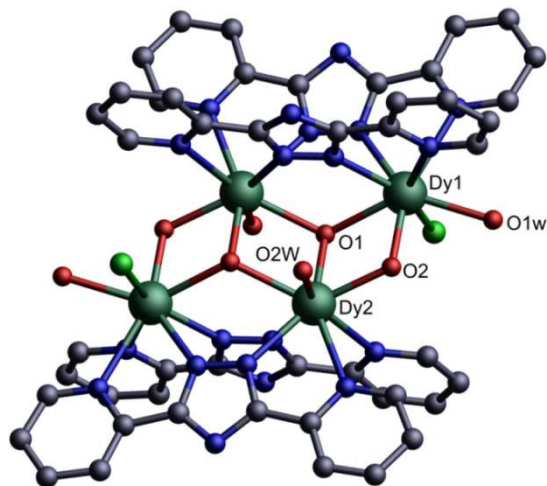


Figure 1. a) The defect-dicubane central core of complex 1. b) Molecule structure without free ions and solvents included in the lattice for 1. Hydrogen atoms are omitted for clarity. Color code: dark green, Dy<sup>III</sup> ion; red, O; blue, N; gray, C.

## Magnetic properties:

**Static magnetic susceptibility:** Variable-temperature dc magnetic susceptibility studies of compounds **1** and **2** have been carried out in an applied magnetic field of 1 kOe over the temperature range 300–2 K. As shown in Figure 2, the room-temperature  $\chi_m T$  values are 55.8 and 56.1 cm<sup>3</sup> K mol<sup>-1</sup> for **1** and **2**, respectively, which are close to the value of 56.6 cm<sup>3</sup> K mol<sup>-1</sup> expected for four uncoupled Dy<sup>III</sup> ions (<sup>6</sup>H<sub>15/2</sub>,  $S = 5/2$ ,  $L = 5$ ,  $J = 15/2$ ,  $g = 4/3$ ).<sup>13b,18</sup> Upon cooling, the  $\chi_m T$  products decrease monotonically to the values of 46 (at ca. 9 K) and 47 cm<sup>3</sup> K mol<sup>-1</sup> (at ca. 16 K) for **1** and **2**, respectively, where they drop abruptly to the minimum of 25.6 (**1**) and 24.8 (**2**) cm<sup>3</sup> K mol<sup>-1</sup>

at 2 K. This behavior is due to the depopulation of the  $M_J$  sublevels of the dysprosium ion that arises from the splitting of the <sup>6</sup>H<sub>15/2</sub> ground term by the crystal field and/or weak Dy<sup>III</sup>...Dy<sup>III</sup> antiferromagnetic interactions.<sup>19</sup> A steep increase is then observed in the isothermal magnetization versus field plots at low temperature and fields. Moreover, without any clear saturation and non-superimposable nature of the curve at larger magnetic fields indicate the presence of strong magnetic anisotropy coming from the ligand-field effects (Figures S1 and S2).

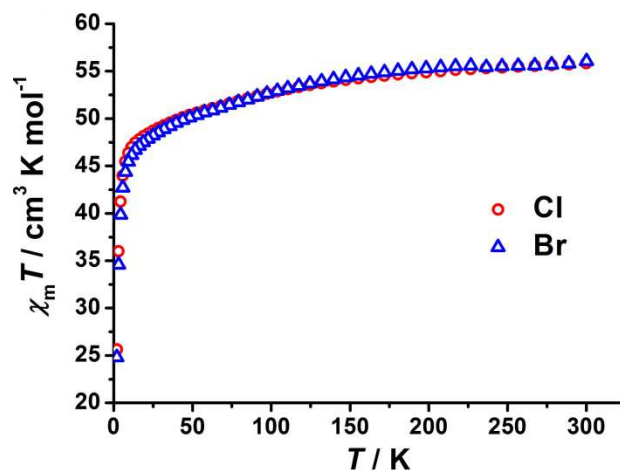


Figure 2. Temperature dependence of the  $\chi_m T$  product at 1 kOe for complex **1** (○) and **2** (△).

**Dynamic magnetic susceptibility:** In order to investigate the magnetic relaxation dynamics of **1** and **2**, alternating-current (ac) magnetic susceptibility measurements as a function of the temperature and frequency were performed on polycrystalline samples in zero applied external dc magnetic fields. The obvious temperature and frequency dependence of the in-phase ( $\chi'$ , Figures 3a, S3) and out-of-phase ( $\chi''$ , Figures 3b, S4) susceptibilities below 30 K confirm the zero-field slow magnetization relaxation and SMM behaviour of complexes **1** and **2**. Upon decreasing temperature, without any obvious increase of  $\chi'$  and  $\chi''$  for both compounds implies the suppressed QTM, which probably due to weak exchange interactions between Dy<sup>III</sup> ions. This observation is consistent with previous studies on lanthanide-based SMMs.<sup>20</sup> The Cole-Cole diagrams for **1** and **2** in the temperature ranges of 9–24 K and 9–25 K (Figures S5, S6) exhibit concurrently semicircular shapes and can be fitted by using the generated Debye model. The  $\alpha$  values fitted are in the ranges of 0.06–0.24 (**1**) and 0.06–0.22 (**2**) that reveal a single dominant relaxation path at higher temperatures, with other pathways becoming competitive at lower temperatures.<sup>21b</sup> The relaxation times extracted from the frequency dependent susceptibility data follow an Arrhenius law ( $\tau = \tau_0 \exp(U_{\text{eff}}/kT)$ ) yielding effective energy barriers for the reversal of the magnetization  $U_{\text{eff}} = 190$  K (**1**) and 197 K (**2**) with pre-exponential factors  $\tau_0 = 2.2 \times 10^{-8}$  s (**1**) and  $1.4 \times 10^{-8}$  s (**2**) (Figure 4). The compound **2** has much longer relaxation time than **1**, which can be seen from the  $\tau$  values for **1** ( $\tau = 0.4$  s) and **2** ( $\tau = 2.4$  s) at 3 K. At

lower temperature, the deviation from the linear relation of relaxation time suggests the presence of other relaxation processes.<sup>21</sup>

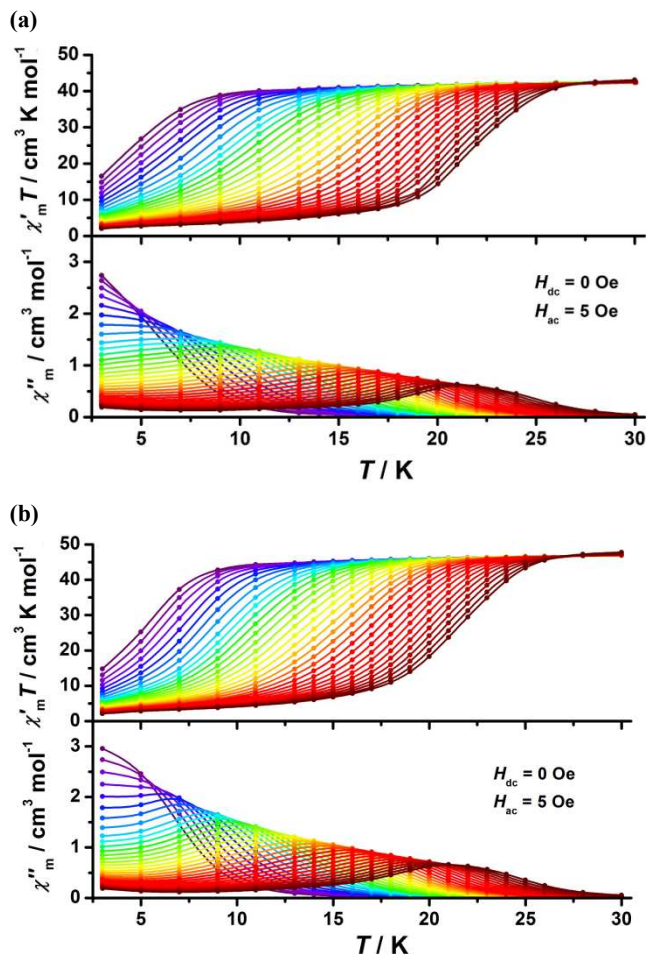


Figure 3. Temperature dependence of the in-phase ( $\chi'$ ) and out-of-phase ( $\chi''$ ) susceptibilities for 1 (a) and 2 (b) below 30 K under a zero dc field.

It should be noted that a toroidal magnetic moment in the absence of conventional total magnetic moment was previously observed in the first 2,2-bpt bridged  $\text{Dy}_4$  SMM,  $([\text{Dy}_4(\mu_3\text{-OH})_2(\mu\text{-OH})_2(2,2\text{-bpt})_4(\text{NO}_3)_4(\text{EtOH})_2])$  (3).<sup>14b</sup> To verify the influence of ligand field on its magnetic anisotropy in the hope of obtaining higher thermal relaxation barrier, only the positions occupied by EtOH molecule and  $\text{NO}_3^-$  around individual  $\text{Dy}^{\text{III}}$  ions of the framework were respectively replaced with  $\text{Cl}^-$  ( $\text{Br}^-$ ) and  $\text{H}_2\text{O}$  molecule in this work. According to the well-known oblate-prolate model,<sup>22</sup> the free ion electron density of the  $\text{Dy}^{\text{III}}$  ion and its ground Kramers doublet with  $M_J = \pm 15/2$  have an oblate shape. This electron density shape is favored by an axial crystal field where the donor atoms with the largest electron densities are best to locate on the perpendicular direction (always close to the shortest Dy-O bond direction) of the transverse plane encompassed by other coordination atoms with smaller electron densities. A reduced interactions between the ligands and f-electron charge clouds will thus be achieved by this kind of arrangement. In these three typically  $\text{Dy}_4$  compounds, the main

anisotropic axes of the ground Kramers doublet on  $\text{Dy}^{\text{III}}$  sites are nearly determined by the shortest Dy-O bond (from  $\mu_2\text{-OH}$ ), which have been already evidenced by the previous *ab initio* calculation in complex 3.<sup>14b</sup> Moreover, the magnetic blocking comes from the local Dy sites rather than exchange interaction. Consequently, it is reasonable to assume that weakening electron densities in the area of the transverse plane by adjusting ligand field can further intensifies the magnetic anisotropy of dysprosium ion. Noted that the magnetic anisotropy in the complexes of 1 and 2 was reinforced prominently which can be supported by apparent variations of energy barrier as well as relaxation time of compounds 1-3 (Table 2). This scenario explains the important role of optimizing ligand field in improving SMM property and consists with the obvious distinction of Dy-X bonds (transverse plane) around  $\text{Dy}^{\text{III}}$  ions under different ligand fields (Table S3).

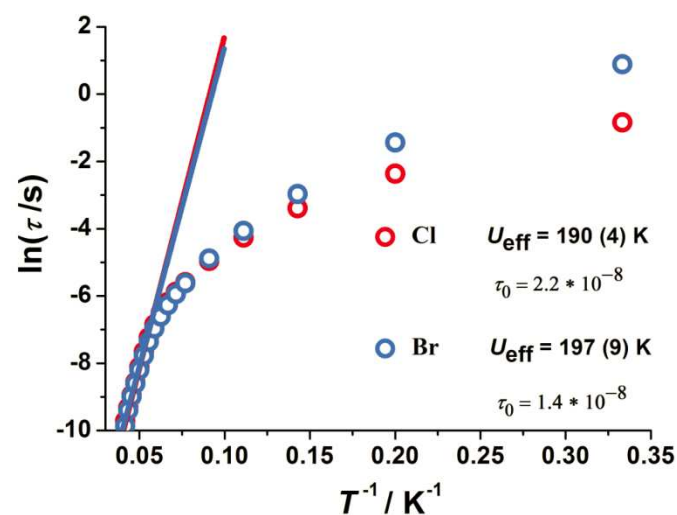


Figure 4. Plots of magnetization relaxation time ( $\ln \tau$ ) versus  $T^{-1}$  for 1 and 2 under a zero-dc field; the solid line represents the best fit to the Arrhenius law.

Table 2. The comparison of SMM properties for complexes 1-3

Compound	1	2	3
$U_{\text{eff}}$ (K)	190	197	80
$\tau_0$ (s)	$2.2 \times 10^{-8}$	$1.4 \times 10^{-8}$	$5.7 \times 10^{-6}$

Hence this will be a good strategy for further optimizing the SMM property in other systems. In addition, the weak intra- and inter-molecular magnetic interactions between  $\text{Dy}^{\text{III}}$  ions of these compounds might also contributed to the SMM behavior.<sup>6b,21b</sup>

## Conclusions

We have shown a good system that the coordination sites of dysprosium ion within a stable  $\text{Dy}_4$  skeleton can be modified purposely. The SMM property in such a typically  $\text{Dy}_4$  cluster can be dramatically boosted by optimizing ligand field around the  $\text{Dy}^{\text{III}}$  ion. In the case of a given coordination configuration, the alteration on donor atoms lie in the area of the transverse plane, such as the choice of coordination atoms with longer bond to  $\text{Dy}^{\text{III}}$  ion or weak crystal field ligand, that can modulate

the ligand field to decrease the electrostatic repulsions between the ligands and f-electron charge clouds, and thus intensify the uniaxial anisotropy. This strategy provides new insight for further enhancing thermal energy barrier in lanthanide-based SMMs.

### Acknowledgements

This work was supported by the “973 Project” (2012CB821704 and 2014CB845602), the NSFC (Grant nos 91122032 and 91422302), the NSF of Guangdong (S2013020013002) and Program for Changjiang Scholars and Innovative Research Team in University of China.

### Notes and references

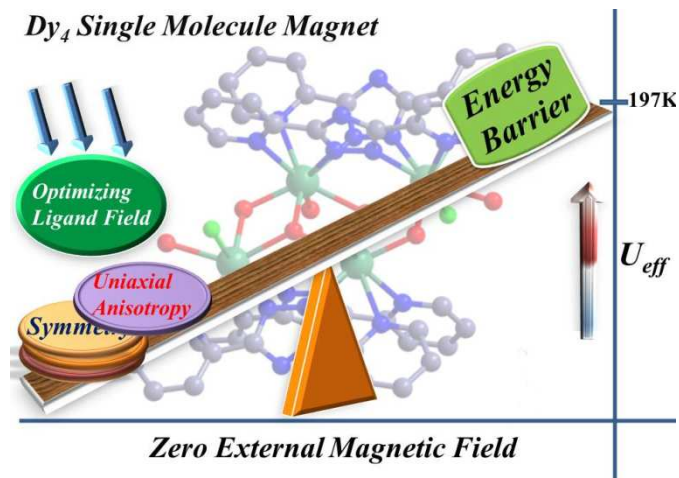
<sup>a</sup> Key Laboratory of Synthetic Bioinorganic Chemistry of Ministry of Education, School of Chemistry and Chemical Engineering, Sun Yat-Sen University, Guangzhou 510275, P. R. China. Fax: (+86)20-8411-2245; E-mail: tongml@mail.sysu.edu.cn

<sup>†</sup> Electronic Supplementary Information (ESI) available: Selected bond lengths and angles for **1** and **2**, variations of Dy-X bonds around Dysprosium ion for compounds **1-3**, *M* versus *H/T* plots for **1** and **2** at indicated temperatures, frequency dependence of the in-phase ( $\chi'$ ) and out-of-phase ( $\chi''$ ) susceptibilities for **1** and **2** below 24 K under a zero dc field and the Cole–Cole plots of compounds **1** and **2** are provided. CCDC: 1046436 and 1046437; crystallographic data in CIF See DOI: 10.1039/b000000x/

- (a) R. Sessoli, D. Gatteschi, A. Caneschi and M. A. Novak, *Nature*, 1993, **365**, 141; (b) M. N. Leuenberger and D. Loss, *Nature*, 2001, **410**, 789.
- X. Feng, J. Liu, T. D. Harris, S. Hill and J. R. Long, *J. Am. Chem. Soc.*, 2012, **134**, 7521.
- (a) M. Murugesu, M. Habrych, W. Wernsdorfer, K. A. Abboud and G. Christou, *J. Am. Chem. Soc.*, 2004, **126**, 4766; (b) A. J. Tasiopoulos, A. Vinslava, W. Wernsdorfer, K. A. Abboud and G. Christou, *Angew. Chem., Int. Ed.*, 2004, **43**, 2117.
- N. Ishikawa, M. Sugita, T. Ishikawa, S.-y. Koshihara and Y. Kaizu, *J. Am. Chem. Soc.*, 2003, **125**, 8694.
- (a) M. A. AlDamen, J. M. Clemente-Juan, E. Coronado, C. Martí-Gastaldo and A. Gaita-Ariño, *J. Am. Chem. Soc.*, 2008, **130**, 8874; (b) S.-D. Jiang, B.-W. Wang, H.-L. Sun, Z.-M. Wang and S. Gao, *J. Am. Chem. Soc.*, 2011, **133**, 4730; (c) P. Zhang, L. Zhang, C. Wang, S. Xue, S.-Y. Lin and J. Tang, *J. Am. Chem. Soc.*, 2014, **136**, 4484; (d) J. J. Le Roy, L. Ungur, I. Korobkov, L. F. Chibotaru and M. Murugesu, *J. Am. Chem. Soc.*, 2014, **136**, 8003.
- (a) C. R. Ganiwet, B. Ballesteros, G. de la Torre, J. M. Clemente-Juan, E. Coronado and T. Torres, *Chem. Eur. J.*, 2013, **19**, 1457; (b) R. J. Blagg, L. Ungur, F. Tuna, J. Speak, P. Comar, D. Collison, W. Wernsdorfer, E. J. L. McInnes, L. F. Chibotaru and R. E. P. Winpenny, *Nat. Chem.*, 2013, **5**, 673; (c) Y.-M. Bing, N. Xu, W. Shi, K. Liu and P. Cheng, *Chem. Asian J.*, 2013, **8**, 1412; (d) N. F. Chilton, *Inorg. Chem.*, 2015, **54**, 2097; (e) N. F. Chilton, C. A. P. Goodwin, D. P. Mills and R. E. P. Winpenny, *Chem. Commun.*, 2015, **51**, 101.
- R. Sessoli and A. K. Powell, *Coord. Chem. Rev.*, 2009, **253**, 2328.
- J.-L. Liu, Y.-C. Chen, Y.-Z. Zheng, W.-Q. Lin, L. Ungur, W. Wernsdorfer, L. F. Chibotaru and M.-L. Tong, *Chem. Sci.*, 2013, **4**, 3310.
- G. Rajaraman, S. K. Singh, T. Gupta and M. Shanmugam, *Chem. Commun.*, 2014, **50**, 15513.
- (a) L. Ungur, J. J. Le Roy, I. Korobkov, M. Murugesu and L. F. Chibotaru, *Angew. Chem., Int. Ed.*, 2014, **53**, 4413; (b) R. J. Blagg, C. A. Murny, E. J. L. McInnes, F. Tuna and R. E. P. Winpenny, *Angew. Chem., Int. Ed.*, 2011, **50**, 6530; (c) J. D. Rinehart, M. Fang, W. J. Evans and J. R. Long, *Nat. Chem.*, 2011, **3**, 538; (d) J. D. Rinehart, M. Fang, W. J. Evans and J. R. Long, *J. Am. Chem. Soc.*, 2011, **133**, 14236.
- I. Oyarzabal, J. Ruiz, J. M. Seco, M. Evangelisti, A. Camón, E. Ruiz, D. Aravena and E. Colacio, *Chem. Eur. J.*, 2014, **20**, 14262.
- (a) K. S. Pedersen, L. Ungur, M. Sigrist, A. Sundt, M. Schau-Magnussen, V. Vieru, H. Mutka, S. Rols, H. Weihe, O. Waldmann, L. Chibotaru, J. Bendix and J. Dreiser, *Chem. Sci.*, 2014, **5**, 1650; (b) F. Habib, G. Brunet, V. Vieru, I. Korobkov, L. F. Chibotaru and M. Murugesu, *J. Am. Chem. Soc.*, 2013, **135**, 13242.
- (a) P.-H. Guo, Y. Meng, Y.-C. Chen, Q.-W. Li, B.-Y. Wang, J.-D. Leng, D.-H. Bao, J.-H. Jia and M.-L. Tong, *J. Mater. Chem. C*, 2014, **2**, 8858; (b) G. Abbas, Y. Lan, G. E. Kostakis, W. Wernsdorfer, C. E. Anson and A. K. Powell, *Inorg. Chem.*, 2010, **49**, 8067; (c) P.-H. Lin, T. J. Burchell, L. Ungur, L. F. Chibotaru, W. Wernsdorfer and M. Murugesu, *Angew. Chem., Int. Ed.*, 2009, **48**, 9489; (d) Y.-N. Guo, G.-F. Xu, P. Gamez, L. Zhao, S.-Y. Lin, R. Deng, J. Tang and H.-J. Zhang, *J. Am. Chem. Soc.*, 2010, **132**, 8538.
- (a) P.-H. Guo, J.-L. Liu, J.-H. Jia, J. Wang, F.-S. Guo, Y.-C. Chen, W.-Q. Lin, J.-D. Leng, D.-H. Bao, X.-D. Zhang, J.-H. Luo and M.-L. Tong, *Chem. Eur. J.*, 2013, **19**, 8769; (b) P.-H. Guo, J.-L. Liu, Z.-M. Zhang, L. Ungur, L. F. Chibotaru, J.-D. Leng, F.-S. Guo and M.-L. Tong, *Inorg. Chem.*, 2012, **51**, 1233; (c) P.-H. Guo, X.-F. Liao, J.-D. Leng and M.-L. Tong, *Acta Chim. Sin.*, 2013, **71**, 173.
- (a) Y.-Z. Zhang, U. P. Mallik, R. Clerac, N. P. Rath and S. M. Holmes, *Chem. Commun.*, 2011, **47**, 7194; (b) Y.-Y. Zhu, T.-T. Yin, S.-D. Jiang, A.-L. Barra, W. Wernsdorfer, P. Neugebauer, R. Marx, M. Dorfel, B.-W. Wang, Z.-Q. Wu, J. van Slageren and S. Gao, *Chem. Commun.*, 2014, **50**, 15090; (c) Y.-Y. Zhu, C. Cui, Y.-Q. Zhang, J.-H. Jia, X. Guo, C. Gao, K. Qian, S.-D. Jiang, B.-W. Wang, Z.-M. Wang and S. Gao, *Chem. Sci.*, 2013, **4**, 1802; (d) Y.-Y. Zhu, X. Guo, C. Cui, B.-W. Wang, Z.-M. Wang and S. Gao, *Chem. Commun.*, 2011, **47**, 8049.
- G. Sheldrick, *Acta Cryst. Sect. A*, 2008, **64**, 112.
- M. Llunell, D. Casanova, J. Cirera, J. M. Bofill, P. Alemany, S. Alvarez, M. Pinsky, D. Avnir, SHAPE v1.1b, Barcelona, 2005.
- P.-P. Yang, X.-F. Gao, H.-B. Song, S. Zhang, X.-L. Mei, L.-C. Li and D.-Z. Liao, *Inorg. Chem.*, 2010, **50**, 720.
- (a) S. K. Langley, B. Moubaraki and K. S. Murray, *Inorg. Chem.*, 2012, **51**, 3947; (b) S. Das, A. Dey, S. Biswas, E. Colacio and V. Chandrasekhar, *Inorg. Chem.*, 2014, **53**, 3417.
- (a) L. F. Chibotaru, L. Ungur and A. Soncini, *Angew. Chem., Int. Ed.*, 2008, **47**, 4126; (b) G. Novitchi, W. Wernsdorfer, L. F. Chibotaru, J. P. Costes, C. E. Anson and A. K. Powell, *Angew. Chem. Int. Ed.*, 2009, **48**, 1614.
- (a) J.-L. Liu, J.-Y. Wu, Y.-C. Chen, V. Mereacre, A. K. Powell, L. Ungur, L. F. Chibotaru, X.-M. Chen and M.-L. Tong, *Angew. Chem., Int. Ed.*, 2014, **53**, 12966; (b) E. Moreno Pineda, N. F. Chilton, R. Marx, M. Dörfel, D. O. Sells, P. Neugebauer, S.-D. Jiang, D. Collison,

- J. van Slageren, E. J. L. McInnes and R. E. P. Winpenny, *Nat Commun.*, 2014, **5**, DOI: 10.1038/ncomms6243.
22. J. D. Rinehart and J. R. Long, *Chem. Sci.*, 2011, **2**, 2078.

## Table of Contents



Two tetranuclear dysprosium clusters with optimized ligand field show enhanced single molecule magnet behaviours. Their high thermal energy barriers with 190 K and 197 K under zero applied external magnetic field are among the highest within the reported tetranuclear lanthanide-based SMMs.